Tunneling effects on the impurity spectral function in coupled asymmetric quantum wires

Marcos R. S. Tavares
Faculdade de Tecnologia da Baixada Santista, CEETPS, Santos, SP 11045-908, Brazil

G.-Q. Hai
Instituto de Física de São Carlos, Universidade de São Paulo, São Carlos, SP 13560-970, Brazil

G. E. Marques
Departamento de Física, Universidade Federal de São Carlos, São Carlos, SP 13565-905, Brazil
(Received 12 April 2003; revised manuscript received 30 June 2003; published 8 October 2003)

The impurity spectral function is studied in coupled double quantum wires at finite temperatures. Simple anisotropy in the confinement direction of the wires leads to finite nondiagonal elements of the impurity spectral function matrix. These nondiagonal elements are responsible for tunneling effects and result in a pronounced extra peak in the impurity spectral function up to temperatures as high as 20 K.

DOI: 10.1103/PhysRevB.68.165304 PACS number(s): 73.50.Gr, 73.21.Hb

I. INTRODUCTION

From a theoretical point of view, it is well known that the Coulomb interaction leads to the Luttinger liquid (LL) behavior of one-dimensional (1D) electron systems. The LL is mostly characterized by the spin-charge separation in the elementary excitation spectrum.[1] However, experimental results concerning inelastic light scattering due to both charge-density (plasmon) and particle-hole (single-particle) excitations in 1D electron systems based on semiconductor quantum wires (SQW's) can be interpreted within the random-phase approximation (RPA) in the framework of the Fermi liquid (FL) theory.[2] Among other issues, the Fermi edge singularity[3] and the band gap renormalization[4,5] in these systems can also be successfully explained within the RPA. As a matter of fact, the resonant inelastic light-scattering experiments in SQW's have been analyzed using both FL and LL theory.[6–8] Recently, a new kind of tunneling spectroscopy in coupled parallel quantum wires in GaAs-based semiconductors was able to check out the Luttinger liquid behavior of the electrons in extremely clean systems at very low temperatures.[9] The differences between the Luttinger and Fermi liquid behaviors turned out to be noticeable in the one-electron spectrum.

So far, no definitive evidence for LL versus FL behavior has been obtained. The puzzle of clarifying the conditions under which the 1D electron system embedded in an SQW behaves as a LL still remains. There have been theoretical suggestions that mechanisms induced by impurity scattering, thermal fluctuations, as well as intersubband scattering can likely suppress the LL behavior.[6,10,11] Effects of the intersubband (or interwire) excitations are believed to disable the LL behavior, provided the system loses its strict one-dimensional character. Moreover, electron intrasubband and intersubband relaxations through slightly impure scattering channels could restore the FL behavior. On the other hand, localized impurity (or defect) induced effects in 1D metallic systems in quantum wires have been extensively studied[12] within both the FL and LL theories. These impurity effects turn out to be related to critical phenomena in the strongly correlated regime and to the x-ray absorption spectrum, where a optical created valence hole is regarded as an impurity.

In this work we are interested in studying the impurity induced optical properties in semiconductor quantum wires which can be helpful in understanding the 1D properties of the electron systems. We focus on the spectral function of a localized valence hole (or a spinless impurity) in two-component coupled double quantum wires at finite temperatures. The considered interaction is of a localized state with a continuum described by a coupled double 1D system with two subbands (or components) filled with electrons. Two parallel wires in the x direction, with zero thickness in the z direction, compose the system. In the y direction, the two wires are of 300 and 200 Å widths, respectively, separated by a 30-Å AlGaAs barrier of 300 meV height. We assume zero thickness in the z direction since the confinement in this direction is much stronger than that in the y direction. The energy gap between the first and the second subbands is $\omega_0 \simeq 5.36$ meV. We consider the impurity localized at the center of the barrier. Such a system is also similar to type-II quantum wire heterostructures, where valence holes are localized between two parallel 1D electron gases.

Our theoretical result indicates that the interwire tunneling induced many-body effects in coupled asymmetric quantum wire systems lead to a nonmonotonic impurity spectral function. A pronounced extra peak appears in the impurity spectral function up to 20 K.

The paper is organized as follows. In Sec. II we present the theory with the working formulas. In Sec. III we provide our numerical results and discussions. We conclude in Sec. IV with a summary.

II. THEORY

A. Interwire Coulomb potential

The anisotropy in the direction perpendicular to the wires leads to very weak tunneling, but it is sensitive enough to produce important effects on both the electron-electron $(e\text{-}e)V^{e\text{-}e}$ and the electron-impurity $(e\text{-}i)V^{e\text{-}i}$ Coulomb inter-

 ©2003 The American Physical Society

actions. The asymmetry leads to nonzero off-diagonal e-e interaction matrix elements of $V^{e\text{-}e}$.[13] These elements represent e-e scattering in which only one of the electrons experiences interwire (or intersubband) transition. In the symmetric situation (two identical wires), however, these off-diagonal matrix elements vanish because the wave functions of the ground and the first excited states are symmetrical and antisymmetrical, respectively, in the confinement direction.

On the other hand, the e-i interaction matrix element related to the interwire transitions is defined as

$$V_{12}^{e\text{-}i}(q)=\frac{2e^2}{\varepsilon_0}\int dy\,\phi_1(y)K_0(q|y|)\phi_2(y), \tag{1}$$

where ε_0 is the static dielectric constant, e the electron charge, $K_0(q|y|)$ the zeroth-order modified Bessel function of the second order, and $\phi_j(y)$ is the electron wave function in the wire (or subband) j. The derivation of this potential is similar to that in Ref. 14, where its quasi-two-dimensional counterpart was calculated. The Bessel function $K_0(q|y|)$ results from the integral in the x direction, which involves the external e-i Coulomb potential

$$V^{\text{ext}}(x,y)=\frac{e^2}{\varepsilon_0}\frac{1}{\sqrt{(x-x_i)^2+(y-y_i)^2}} \tag{2}$$

and the plane wave describing free electrons in that direction. It obviously depends on the impurity position $x_i=y_i=0$, which has been chosen here as the origin of the coordinates. The component $V_{12}^{e\text{-}i}(q)$ represents interwire (intersubband) transitions suffered by the electron as it interacts with the localized impurity. This interaction induces anisotropy (or tunneling) effects on the full impurity spectral function that we investigate in this work. We mention that, for two identical wires, $V_{12}^{e\text{-}i}(q)=0$ due to the fact that $\phi_1(y)$ and $\phi_2(y)$ are symmetrical and antisymmetrical functions of y, respectively.

B. Interwire impurity Greens function

We model the system by an Anderson impurity localized below the continuum of the two subbands ($j=1,2$) in the coupled quantum wires filled with electrons. This approach has been used before in studying optical holes in doped two-dimensional systems at zero temperature.[15–17] We point out that the Hamiltonian presenting the interaction between the impurity and the two-component 1D electron gas can be transformed into a problem of a localized level with energy ε_i and a two-component noninteracting boson (electron-hole pairs). Therefore, we are dealing with an independent boson model which is exactly solvable. The term in the Hamiltonian describing the boson coupling to the impurity is written as

$$H'=d^+d\left[\varepsilon_i+\sum_{\lambda q}V_\lambda^{e\text{-}i}(q)(b_{q\lambda}+b_{-q\lambda}^+)\right], \tag{3}$$

where $b_{\lambda q}^+$ ($b_{\lambda q}$) creates (destroys) a boson in the state $\lambda\equiv(j,j')$ with wave vector q. Here, $V_\lambda^{e\text{-}i}(q)$ is the electron-impurity interaction matrix element. Notice that this coupling occurs only when the impurity state is occupied and $d^+d=1$.

After a canonical transformation of the type $e^S H' e^{-S}$ with

$$S=d^+d\sum_{\lambda q}\frac{V_\lambda^{e\text{-}i}(q)}{\omega_\lambda(q)}(b_{-q\lambda}^+-b_{q\lambda}), \tag{4}$$

the Hamiltonian (3) can be rewritten as

$$H'=d^+d\left(\varepsilon_i-\sum_\lambda\Delta_\lambda\right), \tag{5}$$

where $\Delta_\lambda=\Sigma_q|V_\lambda^{e\text{-}i}(q)|^2/\omega_\lambda(q)$ is the self-energy involving the frequency $\omega_\lambda(q)$ of the boson in the state λ with wave vector q. One may then obtain the impurity Greens function from the Hamiltonian (5). After some algebra, an exact and closed form of the impurity Greens function is obtained:[18]

$$G(t)=-ie^{-it(\varepsilon_i-\Sigma_\lambda\Delta_\lambda)}\prod_\lambda\exp[-\Phi_\lambda(t)], \tag{6}$$

where

$$\Phi_\lambda(t)=\int_0^\infty\frac{d\nu}{\nu^2}R_\lambda(\nu)\{[n_B(\nu)+1](1-e^{-i\nu t})+n_B(\nu)(1-e^{i\nu t})\}, \tag{7}$$

with $n_B(\nu)$ being the Bose distribution function. Feynman's theorem on the disentangling of field operators is employed to determine $G(t)$. The benefit of treating the system within the independent boson model comes when our working formulas are obtained without any approximation.

In Eq. (6), $\Sigma_\lambda\Delta_\lambda$ is the self-energy shift in relation to the impurity energy ε_i. This shift is time independent and has no major effect on the total impurity spectral function other than renormalizing the band-to-band threshold transition energy $\omega_T=\varepsilon_i-\Sigma_\lambda\Delta_\lambda$. For the sake of simplicity, we take $\omega_T=0$ throughout this paper. We focus on the time-dependent self-energy term $\Phi_\lambda(t)$ which requires the boson density of states[18]

$$R_\lambda(\nu)=\frac{1}{\pi}\int\frac{dq}{2\pi}|V_\lambda^s(q,\nu)|^2\text{Im}[\Pi_\lambda(q,\nu)], \tag{8}$$

which determines the shape of the impurity spectral function. In Eq. (8), $V_\lambda^s(q,\nu)$ is the screened e-i Coulomb potential and $\Pi_\lambda(q,\nu)$ is the noninteracting irreducible polarizability function. The screened interaction V_λ^s is obtained from the generalized self-consistent equation

$$V_\lambda^s(q,\nu)=\sum_{\lambda'}[\varepsilon_{\lambda,\lambda'}(q,\nu)]^{-1}V_{\lambda'}^{e\text{-}i}(q), \tag{9}$$

with the dielectric matrix

$$\varepsilon_{\lambda,\lambda'}=\delta_{\lambda\lambda'}-V_{\lambda\lambda'}^{e-e}\Pi_{\lambda'} \tag{10}$$

written within the RPA.

We point out that the formula for the density of states $R_\lambda(\nu)$ has been conveniently chosen in order to take into account elementary excitations (or screening) occurring in the experiment. The quantity $R_\lambda(\nu)$ also plays the role of a density of states for the electron-electron interaction provided it is determined by collective excitations [entering in the calculation via the screened *e-i* potential $V^s_\lambda(q,\nu)$], which remain in the particle-hole excitation continuum where $\mathrm{Im}[\Pi_\lambda(q,\nu)]\neq 0$. It will then depend on the electron density n_e in the sample, since the polarizability Π_λ does. Therefore, in calculating $R_\lambda(\nu)$, we are dealing with a boson density of states, which have been mapped onto elementary excitations in the real electron system.

The elementary excitation spectra of a Fermi system embedded in the biwire structure present the well-known optical $\omega_+(q)$ and acoustic $\omega_-(q)$ plasmon modes corresponding to the in-phase and out-of-phase charge density fluctuations, respectively.[19] The dispersion relations of these modes are obtained through the equation $\det|\varepsilon_{\lambda\lambda'}(q,\omega)|=0$.

We devoted special attention in this work to the element $R_{12}(\nu)$, which is interpreted as the rate of creating interwire electron-hole pairs (bosons) with the electron (hole) being in the wider (narrower) wire. The tunneling between the wires is responsible for $V^{e\text{-}i}_{12}(q)$ and, as a consequence, for $R_{12}(\nu)$. It then leads to the interwire impurity spectral function defined as

$$A_{12}(\omega)=-2\mathrm{Im}\left[\int dt e^{i\omega t} g_{12}(t)\right], \tag{11}$$

where

$$g_{12}(t)=-i\exp[-\Phi_{12}(t)]$$

is the finite temperature impurity Greens function involving the electronic transitions between the wires. The impurity spectral function in 3D systems at zero temperature diverges as a power law at $\omega\rightarrow\omega_T$. This divergency is due to the so-called orthogonality catastrophe involving the overlap between the initial (without impurity) and final (with impurity) many-body states.[20] Here, the Bose distribution function $n_B(\omega)$, governing the particle-hole excitations at finite temperatures, plays the important role of being responsible for the behavior of $A_{12}(\omega)$ as $\omega\rightarrow 0$.

III. NUMERICAL RESULTS

In Fig. 1 we show $R_{12}(\nu)$ at different temperatures for the total charge density $n_e=10^6$ cm^{-1}. As discussed above, Eq. (8) indicates that the screened *e-i* potential $V^s_{12}(q,\nu)$ in the interwire particle-hole continuum, where $\mathrm{Im}[\Pi_{12}(q,\nu)]\neq 0$, determines the interwire density of states $R_{12}(\nu)$. On the other hand, the weak interwire particle-hole excitations in the present system only result in partial Landau damping on the plasmon modes as we discussed in Ref. 13. Therefore, the survived optical $\omega_+(q)$ and acoustic $\omega_-(q)$ plasmon modes in this region are a dominant contribution to $V^s_{12}(q,\nu)$ and, consequently, in determining the $R_{12}(\nu)$. In order to understand that, we show in Fig. 2 the intrawire and interwire particle-hole excitation spectra along with the plasmon dispersion relations of the optical and acoustic modes in the system with $n_e=10^6$ cm^{-1} at zero temperature. The corresponding $R_{12}(\nu)$ is given by the solid curve in Fig. 1. Clearly, there are well defined borders of the interwire particle-hole continuum at zero temperature. The well shaped

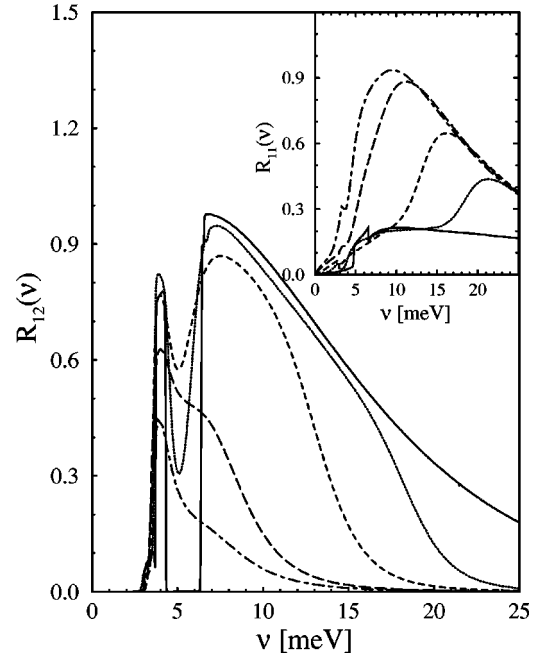

FIG. 1. The rate $R_{12}(\nu)$ for $n_e=10^6$ cm^{-1} at different temperatures: $T=0$ K (solid line), $T=5$ K (dotted line), $T=10$ K (short-dashed line), $T=20$ K (dashed line), and $T=25$ K (dash-dotted line). The inset shows the intrawire rate $R_{11}(\nu)$ for the same temperature values.

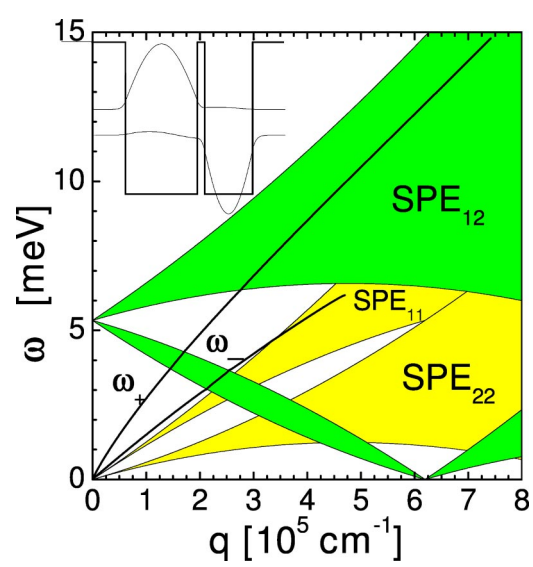

FIG. 2. (Color online) Dispersion relations of the optical $\omega_+(q)$ and acoustic $\omega_-(q)$ plasmon modes with $n_e=10^6$ cm^{-1} . Shaded areas indicate the intrawire and interwire particle-hole excitation continua. The inset shows the wire structure and the wave functions of the ground and first excited states.

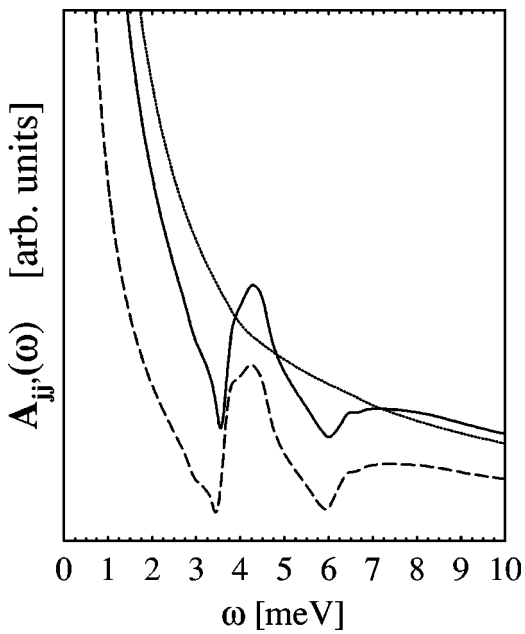

FIG. 3. The elements $A_{jj'}(\omega)$ at temperature $T=2$ K. Here, $n_e=10^6$ cm^{-1}.

$R_{12}(\nu)$ follows the optical and acoustic branches entering and leaving each continuum region. The acoustic (optical) mode enters and leaves the lower interwire particle-hole continuum region at $\omega_- \simeq 3.0$ and 3.8 meV ($\omega_+ \simeq 3.7$ and 4.3 meV), respectively. The optical one enters the higher interwire particle-hole continuum region at $\omega_+ \simeq 6.3$ meV. In comparison with the plasmon dispersions, our calculation indicates that $R_{12}(\nu)$ is dominated by the acoustic and optical plasmon branches which remain in the interwire particle-hole continuum. We address the fact that, in calculating $R_{12}(\nu)$, we are dealing with an interwire boson density of states, which have been mapped onto elementary excitations in the Fermi system.

For the sake of completeness, we show the intrawire element $R_{11}(\nu)$ in the inset of Fig. 1 for the same temperature range. The rate $R_{11}(\nu)$ is dominated by the intrawire particle-hole excitations. But the partially damped acoustic plasmon mode in the intrawire particle-hole excitation continuum has a small contribution to $R_{11}(\nu)$ in our asymmetric system. We also show that, quantitatively, $R_{12}(\nu)$ is larger than $R_{11}(\nu)$ at very low temperatures. Consequently, it dominates the full impurity spectral function at low temperatures. With increasing temperature, $R_{12}(\nu)[R_{11}(\nu)]$ decreases (increases)and the interwire effects carried by $R_{12}(\nu)$ are suppressed by $R_{11}(\nu)$. Moreover, the function $R_{12}(\nu)$ behaves differently compared to $R_{11}(\nu)$ which is roughly a slowly varying function. The abrupt increase in $R_{12}(\nu)$ leads to a specific structure in the impurity spectral function. We also found that the elements $R_{22}(\nu)$ and $R_{21}(\nu)$ are of negligible contribution due to the small probability of creating electron-hole pairs whose electrons are found in the narrower wire.

In Fig. 3, the dotted and dashed lines show $A_{jj'}(\omega)$ for $(j,j')=(1,1)$ and $(j,j')=(1,2)$, respectively, at $T=2$ K. The full spectrum (solid line) should be observed experimentally via photoemission or photocurrent spectroscopy and are proportional to the impurity density of states involving elementary excitations mostly due to the wider quantum wire. The interwire tunneling induced effects as discussed above reflect on the nondiagonal element $A_{12}(\omega)$. We see structures in the spectral function $A_{12}(\omega)$ in which the dip and peak correspond to the behavior of $R_{12}(\nu)$. These structures represent the contribution coming from interwire boson excitations, which decrease as the temperature increases.

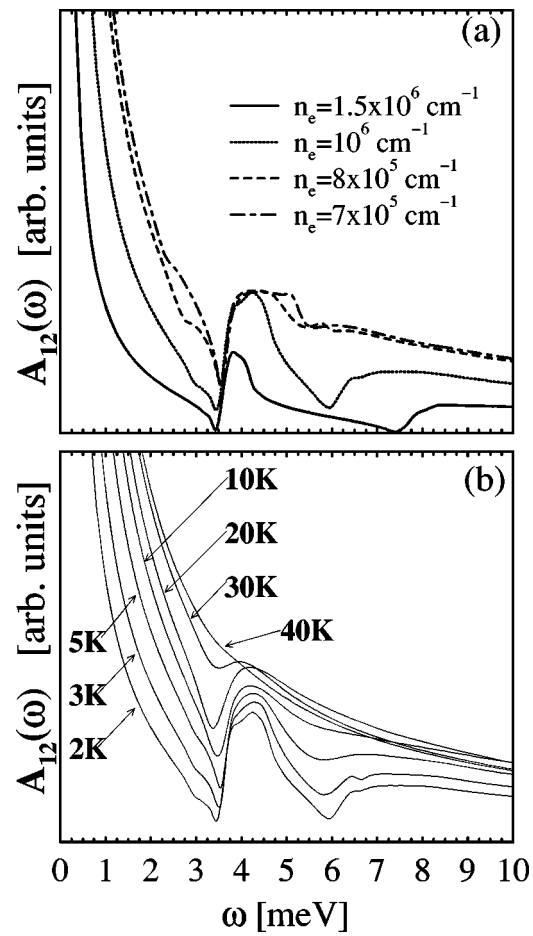

FIG. 4. (a) The interwire element $A_{12}(\omega)$ at temperature $T=2$ K for different electron densities n_e. (b) The interwire element $A_{12}(\omega)$ for $n_e=10^6$ cm^{-1} at different temperatures.

In Fig. 4(a), we show $A_{12}(\nu)$ at temperature $T=2$ K for different charge densities n_e. The figure clearly shows the effects due to interwire particle-hole excitations and their dependence on the total charge density in the sample. As n_e decreases, the narrower wire becomes less populated and the shoulders in the figures get affected. In Fig. 4(b), we show the temperature evolution of $A_{12}(\omega)$ for $n_e=10^6$ cm^{-1}. Although the temperature suppresses the interwire boson excitations, the effects due to interwire interaction are observable in our calculation up to $T=30$ K. Moreover, the Boson distribution function $n_B(\omega)$, governing the interwire self-energy propagator $\Phi_{12}(t)$ at finite temperatures, leads to the divergency in $A_{12}(\omega)$ for $\omega \to 0$.

IV. SUMMARY

In summary, we have studied the nondiagonal (interwire) element of the spectral function matrix of a localized impurity in coupled double quantum wires. We show that the tunneling between the two asymmetric wires induces interwire particle-hole excitation effects leading to a pronounced peak in the impurity spectral function up to 20 K which should be observable in the photoemission or photocurrent spectroscopy. We finally remark that experimental observations of these effects could serve as a signature of one-dimensional FL in the proposed system.

ACKNOWLEDGMENTS

This work was supported by FAPESP, the research foundation agency of the state of São Paulo, Brazil. G.Q.H. and G.E.M. acknowledge CNPq from Brazil for financial support.

[1] J. Voit, Rep. Prog. Phys. **58**, 977 (1995).
[2] A. Goñi, A. Pinczuk, J.S. Weiner, J.M. Calleja, B.S. Dennis, L.N. Pfeiffer, and K.W. West, Phys. Rev. Lett. **67**, 3298 (1991).
[3] F.J. Rodriguez and C. Tejedor, Phys. Rev. B **47**, 1506 (1993).
[4] E.H. Hwang and S. Das Sarma, Phys. Rev. B **58**, R1738 (1998).
[5] H. Akiama *et al.*, Solid State Commun. **122**, 169 (2002); and K. Guven, B. Tanatar, and C.R. Bennet, J. Phys.: Condens. Matter **12**, 2031 (2000).
[6] B.Y.-K. Hu and S. Das Sarma, Phys. Rev. B **48**, 5469 (1993).
[7] B. Kramer and M. Sassetti, Phys. Rev. B **62**, 4238 (2000); and M. Sassetti and B. Kramer Phys. Rev. Lett. **80**, 1485 (1998).
[8] D.W. Wang, A.J. Millis, and S. Das Sarma, Phys. Rev. B **64**, 193307 (2001); and D.W. Wang and S. Das Sarma, *ibid.* **65**, 035103 (2002).
[9] O.M. Auslaender *et al.*, Science **295**, 825 (2002).
[10] Marcos R. S. Tavares, S. Das Sarma, and G.-Q. Hai, Phys. Rev. B **63**, 045324 (2001).
[11] F. Capurro, M. Polini, and M.P. Tosi, Physica B **325**, 287 (2003).
[12] Y. Tsukamoto, T. Fujii, and N. Kawakami, Eur. Phys. J. B **5**, 479 (1998), and references therein.
[13] Marcos R. S. Tavares and G.-Q. Hai, J. Phys.: Condens. Matter **13**, 6421 (2001).
[14] G.-Q. Hai, F.M. Peeters, N. Studart, and G.E. Marques, Superlattices Microstruct. **25**, 185 (1999).
[15] P. Hawrylak, Phys. Rev. B **42**, 8986 (1990).
[16] P. Hawrylak, Phys. Rev. B **44**, 3821 (1991); *ibid.* **44**, 6262 (1991); *ibid.* **44**, 11236 (1991).
[17] M. Tavares, C. Tejedor, and G.E. Marques, Phys. Rev. B **56**, 9753 (1997).
[18] For a review, see G. D. Mahan, *Many Particle Physics*, 2nd ed. (Plenum, New York, 1981). Details for detemining the impurity Greens function can be seen in Sec. IV c, while Sec. VIII c shows the definition for $R_\lambda(\nu)$.
[19] Marcos R. S. Tavares and G.-Q. Hai, Phys. Rev. B **61**, 7564 (2000).
[20] G.D. Mahan, Phys. Rev. **63**, 612 (1967); G.D. Mahan, *ibid.* **153**, 882 (1967); and M. Combescot and P. Nozières, J. Phys. (France) **32**, 913 (1971).